

A generalized model of maximizing the sensitivity in intensity-interrogation surface plasmon resonance biosensors

Chung-Tien Li,¹ Ta-Jen Yen,^{1,2,*} and How-foo Chen^{3,*}

¹Department of Materials Science and Engineering, National Tsing Hua University, Hsinchu 30013, Taiwan, R.O.C.

²Institute of NanoEngineering and MicroSystems, National Tsing Hua University, Hsinchu 30013, Taiwan, R.O.C.

³Institute of Biophotonics Engineering, National Yang Ming University, Taipei 112, Taiwan, R.O.C.
hfchen3@ym.edu.tw

* tjyen@mx.nthu.edu.tw

Abstract: Intensity interrogation of surface plasmon resonance (IISPR) biosensors possesses the greatest sensitivity beyond other interrogations and is operated at a fixed incident angle to enable real-time analysis without time delay, so that it promises excellent performance in biological/chemical detection and SPR imaging systems. Here we provide a general model to describe its sensitivity based on Lorentz equation and unveil the relation between the sensitivity and the metal thickness. This model presents the dependency between sensitivity and metal thickness, and the optimal thickness of gold layers to maximize the sensitivity in our experiment is 53 nm that agrees well in both measurement and simulation. This general model can be further applied in other intensity-interrogation SPR configurations as a design rule for sensing and imaging applications.

©2009 Optical Society of America

OCIS codes: (130.6010) Sensors; (240.6680) Surface plasmons; (240.0310) Thin films; (000.4430) Numerical approximation and analysis

References and links

1. E. Gizeli, and C. R. Lowe, "Immunosensors," *Curr. Opin. Biotechnol.* **7**(1), 66–71 (1996).
2. J. M. McDonnell, "Surface plasmon resonance: towards an understanding of the mechanisms of biological molecular recognition," *Curr. Opin. Chem. Biol.* **5**(5), 572–577 (2001).
3. H. Raether, *Surface plasmons on smooth and rough surfaces and on gratings* (Springer-Verlag, 1988).
4. J. Homola, S. S. Yee, and G. Gauglitz, "Surface plasmon resonance sensors: review," *Sensor Actuat. Biol. Chem.* **54**, 3–15 (1999).
5. B. Ran, and S. G. Lipson, "Comparison between sensitivities of phase and intensity detection in surface plasmon resonance," *Opt. Express* **14**(12), 5641–5650 (2006).
6. T. Zacher, and E. Wischerhoff, "Real-Time Two-Wavelength Surface Plasmon Resonance as a Tool for the Vertical Resolution of Binding Processes in Biosensing Hydrogels," *Langmuir* **18**(5), 1748–1759 (2002).
7. V. Kanda, J. K. Kariuki, D. J. Harrison, and M. T. McDermott, "Label-Free Reading of Microarray-Based Immunoassays with Surface Plasmon Resonance Imaging," *Anal. Chem.* **76**(24), 7257–7262 (2004).
8. K. F. Giebel, C. Bechinger, S. Herminghaus, M. Riedel, P. Leiderer, U. Weiland, and M. Bastmeyer, "Imaging of cell/substrate contacts of living cells with surface plasmon resonance microscopy," *Biophys. J.* **76**(1), 509–516 (1999).
9. E. M. Yeatman, "Resolution and sensitivity in surface plasmon microscopy and sensing," *Biosens. Bioelectron.* **11**(6-7), 635–649 (1996).
10. F. C. Chien, and S. J. Chen, "A sensitivity comparison of optical biosensors based on four different surface plasmon resonance modes," *Biosens. Bioelectron.* **20**(3), 633–642 (2004).
11. H. F. Chen, C. C. Gong, and T. J. Yen, "An innovative surface plasmon resonance biosensor with stationary light source and detection system capable of adjustable incident angles with large range," (to be submitted).
12. E. Fontana, "Thickness optimization of metal films for the development of surface-plasmon-based sensors for nonabsorbing media," *Appl. Opt.* **45**(29), 7632–7642 (2006).
13. J. S. Maier, S. A. Walker, S. Fantini, M. A. Franceschini, and E. Gratton, "Possible correlation between blood glucose concentration and the reduced scattering coefficient of tissues in the near infrared," *Opt. Lett.* **19**(24), 2062–2064 (1994).

1. Introduction

Interactions among biological molecules offer considerable dynamic information for medical diagnostics, life science, food safety, and drug developments; consequently, a variety of biosensors has been developed in studying the respective antibody-antigen interactions, DNA hybridizations, cancer cells monitoring, blood glucose detection, and so on [1]. Foremost among those biosensors, it is the surface plasmon resonance (SPR) biosensor operated by detecting the local change of refractive indices, to exhibit practical advantages of label-free detection, real-time monitoring, small amount of required analytes, and excellent sensitivity [2]. Surface plasmon resonance (SPR) is a collective oscillation of electrons propagating along the interface between metal and dielectric layers, in which the resonance condition is extremely sensitive to a slight variation of refractive indices of dielectric environments to achieve powerful biological and chemical analysis by measuring the shift of corresponding optical signals such as resonant angles, resonant wavelengths, fluctuations of phase and intensity [3]. As a result, SPR biosensors can be classified into four interrogations— angular, wavelength, phase, and intensity interrogations [4].

Among these four interrogations, intensity interrogation demonstrates a great sensitivity—for instance, more than two orders of magnitude higher than angular interrogation demonstrated in both simulated and experimental works [5]. More importantly, detection in the intensity interrogation records optical reflectance at a fixed incident angle that enables further advantages of eliminating lossy noises, avoiding rough transitions and achieving real-time measurement, leading the intensity interrogation par excellence beyond other SPR techniques in dynamic monitoring [6]. In addition to stationary configuration, the intensity mode only requires a simpler optical setup so that currently it is readily employed to construct an SPR imaging system [7], in particular for multi-array detection [7] and activity observation of living cells [8].

Although the intensity interrogation exhibits various merits aforementioned, surprisingly, there were few studies to discuss the intrinsic properties of intensity interrogation SPR (IISPR) biosensors. A recent discussion by Yeatman *et al.* numerically illustrated that the sensitivity depends on the extreme reflectance slope, which can be predicted by two damping factors, internal damping and radiation damping [9]. More recently, Chen *et al.* numerically expressed the sensitivity of IISPR with the effect of the refractive index and thickness of the biomolecular layer [10]. In this letter, we report a generalized model of thickness-dependent sensitivity for IISPR biosensors to manifest the relation between the sensitivity and gold film thicknesses, and specify an optimal gold thickness to maximize the sensitivity in IISPR biosensors. This proposed model can be further applied in other IISPR systems, such as different incident sources and sensing metals, providing a design rule for sensing and imaging applications.

2. Materials and methods

2.1 Surface plasmon resonance system

In this experiment, we developed a homemade SPR system with the stationary light source and detection system to achieve adjustable incident angles for greater scanning ranges [11]. As illustrated in Fig. 1, we applied a 3 mW laser diode with 633 nm in wavelength as the light source, and a linear polarizer in front of the laser to improve the extinction ratio of the polarization state up to $10^5:1$. A half-wave plate was used to properly adjust the ratio of the p-wave and s-wave for the excitation of surface plasmon (SP) and as the reference beam to normalize of the laser instability on intensity. Different from the conventional optical setup performing angular interrogation method, we fixed the laser and the detection system but the incident angle can be changed through the employment of a paired off-axis parabolic mirrors and a set of rectangular mirrors. Since the laser and detector were fixed at all time, the unstable factor by changing incident angles in conventional SPR biosensors will be eliminated to significantly enhance and the stability of the SPR system. Besides, we fabricated six different thicknesses of gold films (47, 50, 53, 56, 59 and 62 nm, respectively)

by an electron-beam evaporation process, with 3 nm in interval. For the measurement of IISPR, first we swept the incident angle from 45° to 65° to obtain the SPR curve of water and then calculated the first-order differentiation of the original SPR curve. After that, the rectangular mirror moved to the corresponding position where the extreme slope happens. Subsequently, glucose solutions with different concentrations were introduced into the flow channel, and the photodiode recorded the optical intensity variation in real time.

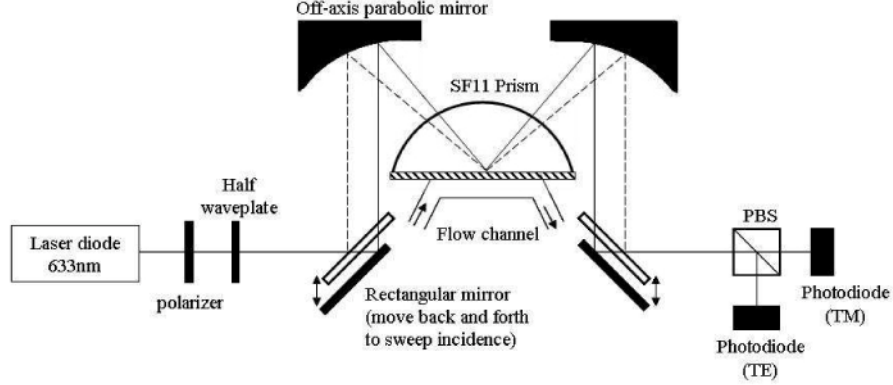


Fig. 1. Illustrated optical setup of a homemade SPR biosensor with stationary light source and detection system, achieving adjustable incident angles for greater scanning ranges

2.2 Sensitivity formula of intensity interrogation SPR biosensor

Once introducing the detected analyte into the IISPR system, the change of reflectance is collected immediately for the succeeding analysis. We expand its sensitivity (dR/dn_a) into two terms in the following,

$$S_{intensity} = \frac{dR}{dn_a} = \frac{dk_x}{dn_a} \times \frac{dR}{dk_x} \quad (1)$$

where R denotes the reflectance of the SPR curve, n_a the refractive index of the analyte, and k_x (i.e., $k_0 \times \sin\theta$) the tangential wave vector along the interface between the metal film and the analyte. In Eq. (1) the first term dk_x/dn_a is invariant as the incident wavelength and the sensing metal are chosen; yet the second term dR/dk_x , will be further modified by changing the thickness of metals to maximize the sensitivity in an IISPR biosensor. In addition, the reflectance R of the SPR curve can be described by the Lorentz equation [3, 9] as below,

$$R = 1 - \frac{4\Gamma_i\Gamma_{rad}}{\left[k_x - (k_{SP}^0 + \Delta k_x)\right]^2 + (\Gamma_i + \Gamma_{rad})^2} \quad (2)$$

where Γ_i represents the internal damping, Γ_{rad} the radiation damping, k_{SP}^0 the intrinsic wave vector of SPR, and Δk_x the corrected term based on the backscattering condition.

Finally, by combining Eq. (1) and (2), we deduce a generalized model to describe the sensitivity of an IISPR biosensor and unveil the relation between the sensitivity and the metal thickness in the following.

$$S_{intensity} = -\frac{3\pi\sqrt{3}}{\lambda} \frac{\varepsilon_m^2}{(\varepsilon_m + n_a^2)\sqrt{\varepsilon_m^2 + \varepsilon_m n_a^2}} \frac{\Gamma_i\Gamma_{rad}}{(\Gamma_i + \Gamma_{rad})^3} \quad (3)$$

where ε_m is the real part of metal's dielectric constant. In this generalized model, the first term in Eq. (1), dk_x/dn_a , is calculated by the first-order differentiation of the SPR dispersion

equation, and meanwhile the second term in Eq. (1), dR/dk_x , essentially proportional to the slope of the SPR curve (i.e., $dR/d\theta$), evaluated at its maximum by using the formula,

$$k_x - (k_{SP}^0 + \Delta k_x) = -\frac{\Gamma_i + \Gamma_{rad}}{\sqrt{3}} \quad (4)$$

which is the formula of setting the second-order differentiation of the Lorentz equation to be zero. Notice that a negative sign is chosen in Eq. (3) because in real case the extreme slope of SPR curves appears at lower incident angles to own less loss. Obviously, these two kinds of damping fundamentally determine the performance of an IISPR sensor—the internal damping (Γ_i) denotes the intrinsic absorption in SPR that is impervious to the incident angle and the thickness of metal layers, but the radiation damping (Γ_{rad}) that stems from the backscattered radiation loss in the metal layer indicates a significant dependence to the incident angle and the thickness of metal layers aforementioned. As a result, Eq. (3) paves a route toward maximizing the sensitivity of an IISPR biosensor by deliberately employing an optimal thickness of metals at a fixed incident angle.

3. Results and discussion

3.1 Theoretical calculations of SPR depend on metal thickness

Since the SPR curve substantially depends on the internal damping and radiation damping, its first-order differentiation certainly becomes a function of these two damping terms as well. Fig. 2 (a) shows the first-order differentiation of the measured SPR curves about the analyte of distilled water for different thicknesses of gold layers, in which the incident angle to acquire the extreme slope always appears at the one smaller than the resonance angle instead of the larger one to avoid the greater absorption at the larger incidence [12]. Besides, we also simulate both the internal and radiation damping versus incident angles for various thicknesses of gold layers. As shown in Fig. 2(b), all the internal damping (black dashed line) remains at $1.68 \times 10^5 \text{ m}^{-1}$ owing to the fact that the intrinsic absorption of metals is independent with their thicknesses; nevertheless, the radiation damping (color solid lines) decreases as increasing the metal thickness. Consequently, among six thicknesses in Fig. 2, it is the 53 nm-thick gold layer to demonstrate the extreme value of slopes (i.e., the smallest value, -0.499) in which the radiation damping equals a half of the internal damping, leading to the maximum sensitivity [9]. Notice that the incident angle of showing the extreme slope differs in each thickness, so that it is necessary to measure the analyte at the respective incident angle for different thicknesses.

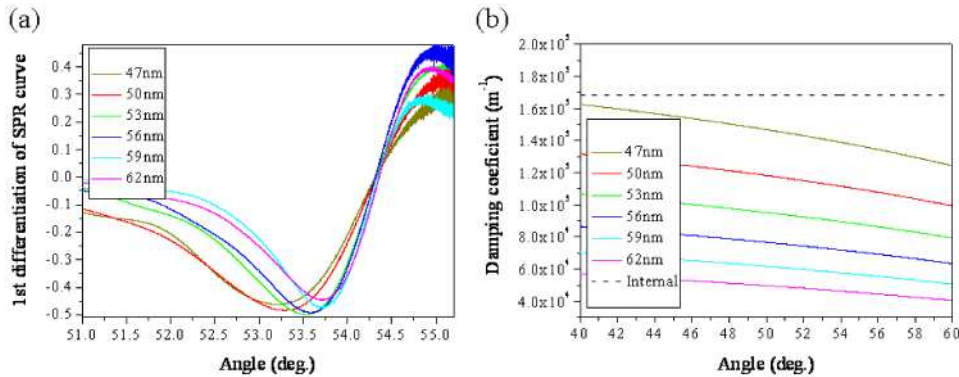


Fig. 2. (a) The first-order differentiation of the measured SPR curves about the analyte of distilled water for different thicknesses of gold layers (47, 50, 53, 56, 59 and 62 nm, respectively). (b) Simulation results of internal damping and radiation damping for different gold thicknesses ($\epsilon_{Au} = -10.98 + 1.4i$ was used in simulation).

3.2 Real-time detection of different Au thicknesses

Next, a real-time detection by an IISPR biosensor was given to verify this thickness-dependent model. Fig. 3 shows the dynamic monitoring of glucose solutions, in which the detection angle is 0.08° greater than the angle with extreme slope to obtain a better sensitivity and linear variation in dynamic measurements. First, double distilled water was first introduced into flow channels as a reference. Next, after the signal of the SPR curve is stable, glucose solutions with 0.05 M and 0.1 M concentrations were injected as the targeting analytes whose refractive indices are estimated through the equation $n = 1.325 + 1.515 \times 10^{-4} \times C$, where n represents the refractive index of glucose solutions, C is the concentration in grams per liter [13], and molecular weight of glucose is 180.16 g/Mol. Based on such a setup, the optical signal is captured immediately without time-delay process due to the fixed angle detection, resulting in a smooth dynamic transition curve beyond other interrogations [6]. As expected by our proposed model, the intensity shift significantly varies along with the thickness of gold layers since the sensitivity in IISPR biosensor linearly depends on the slope of the SPR curve according to Eq. (1). More importantly, the case of 53-nm thick gold layer manifests the greatest intensity shift (i.e., the greatest sensitivity) beyond other cases and such a result agrees well with the measurement and simulation in Fig. 2.

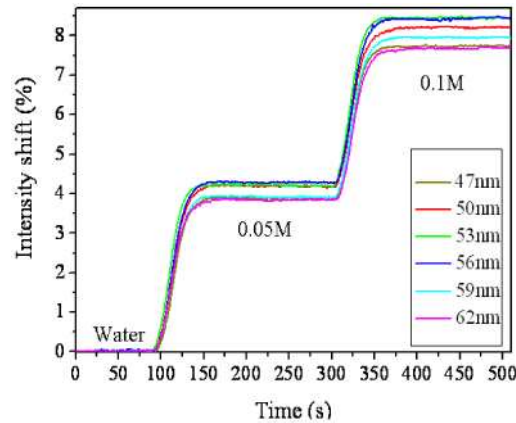


Fig. 3. Dynamic monitoring of glucose solutions based on different gold thicknesses. The incidence in each metal thickness was 0.08° greater than the angle with extreme slope to obtain a better sensitivity and linear variation in dynamic measurements. Besides, the glucose solutions with 0.05 M and 0.1 M concentrations were introduced into the flow channel sequentially.

In addition, we further calculate the sensitivity based on Eq. (3) to compare with the measured one. For each metal thickness, four to five samples were calculated and tested, as shown in Fig. (4). The calculated and experimental sensitivity presents a parabolic relation with the metal thickness, and both results consistently indicate the maximum sensitivity in the case of a 53 nm-thick gold layer. The relation between sensitivity and metal thickness can be explained by the coupling efficiency and the loss within the SPR curve. Since the sensitivity of intensity interrogation linearly depends on the extreme slope of the SPR curve according to Eq. (1), which is regarded as the ratio of the curve depth and width. The depth of SPR curves relates to the coupling efficiency, depending on the metal thickness to exhibit a parabolic relationship with an optimal value to have maximum depth (i.e., zero reflection); yet the width of SPR curves directly relates to the sum of internal and radiation damping, which is decreased with the thicker metals according to Fig. 2(b). By considering the two dependencies, the sensitivity is maximized at the thickness slightly greater than the best coupling thickness. These two curves of thickness-dependent sensitivity exhibit the same trend in spite of a slight offset due to the approximation of the applied Lorentz equation. Basically the Lorentz equation assumes $|\epsilon_{\text{metal}}^{\text{real}}| \gg 1$ and $|\epsilon_{\text{metal}}^{\text{real}}| \gg |\epsilon_{\text{metal}}^{\text{imaginary}}|$, which deviates

from the real cases [3]; moreover, it expresses the SPR curve in a symmetric fashion to ignore a significant protuberance near the SPR dip corresponding to the critical angle, and such critical angle protuberance will influence the slope of the SPR curve during measurements. Therefore, a slight underestimation in calculation surfaces as shown in Fig. 4.

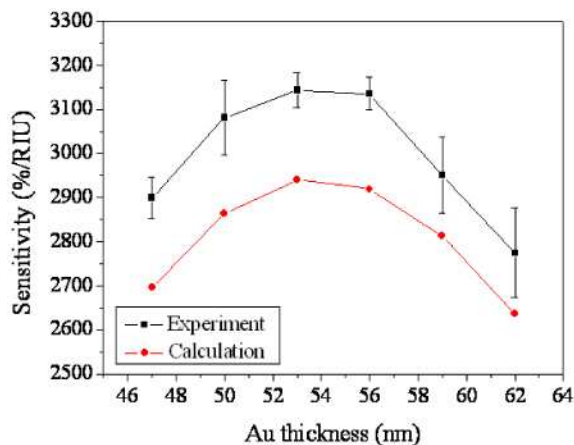


Fig. 4. Sensitivity comparison among different gold thicknesses. Four to five samples were examined in each thickness, and the maximum sensitivity happens in case of a 53 nm-thick gold layer, which coincides with the numerical calculation results.

4. Conclusion

In conclusion, in this work we develop a generalized model to describe the sensitivity in an intensity interrogation SPR (IISPR) biosensor. The sensitivity substantially depends on the internal damping and radiation damping, which are mainly determined by the thickness of metals in the intensity interrogation system. According to this model, we show that in case of a 53 nm-thick gold layer under a 633 nm incidence, the radiation damping equals a half of the internal damping, leading to the maximum sensitivity. Such a result is also verified by real-time detection of glucose solutions, measured by a homemade SPR system with the stationary light source and detection system to achieve adjustable incident angles for greater scanning ranges. In short, this thickness-dependent model validates in both simulation and experiments and can be further applied in other IISPR systems, regardless of metal species, prisms, and the wavelength of light sources, providing a design rule for practical sensing and imaging applications.

Acknowledgements

This work was supported by National Science Council (NSC) and Chang-Gung Memorial Hospital (98N2430E1), and National Science Council (95B0508J4).